Hindawi
Advances in Materials Science and Engineering
Volume 2017, Article ID 2316347, 13 pages
https://doi.org/10.1155/2017/2316347

Research Article

Mechanical Properties of Fiber-Reinforced Concrete Using Composite Binders

Roman Fediuk, Aleksey Smoliakov, and Aleksandr Muraviov

Far Eastern Federal University, Vladivostok 690950, Russia

Correspondence should be addressed to Roman Fediuk; roman44@yandex.ru

Received 14 June 2017; Revised 12 September 2017; Accepted 19 September 2017; Published 26 October 2017

Academic Editor: Rishi Gupta

This paper investigates the creation of high-density impermeable concrete. The effect of the "cement, fly ash, and limestone" composite binders obtained by joint grinding with superplasticizer in the varioplanetary mill on the process of structure formation was studied. Compaction of structure on micro- and nanoscale levels was characterized by different techniques: X-ray diffraction, DTA-TGA, and electron microscopy. Results showed that the grinding of active mineral supplements allows crystallization centers to be created by ash particles as a result of the binding of $Ca(OH)_2$ during hardening alite, which intensifies the clinker minerals hydration process; the presence of fine grains limestone also leads to the hydrocarboaluminates calcium formation. The relation between cement stone neoplasms composition as well as fibrous concrete porosity and permeability of composite at nanoscale level for use of composite binders with polydispersed mineral supplements was revealed. The results are of potential importance in developing the wide range of fine-grained fiber-reinforced concrete with a compressive strength more than 100 MPa, with low permeability under actual operating conditions.

1. Introduction

Concrete on cementitious binder and natural aggregates is widely used as structural material in construction industry. Worldwide, the large-capacity ash waste and crushing of the rocks are generated as a result of activity of the fuel and energy sector and mining industry enterprises. It seems necessary to optimize the processes of concrete mixtures structure formation by using industrial waste. Traditional types of concrete have insufficient properties of gas permeability and vapor permeability. At the same time, it is necessary to improve the strength and deformability quality of composite to achieve fine-grained fiber-reinforced concrete.

Leading scientific schools in the field of building materials science have developed a number of concrete types with enhanced operational properties.

Textile-reinforced concrete is a type of reinforced concrete in which the usual steel reinforcing bars are replaced by textile materials. Materials with high tensile strengths with negligible elongation properties are reinforced with woven or nonwoven fabrics. The fibers used for making the fabric are of high tenacity like Jute, glass fiber, Kevlar, polypropylene, polyamides (nylon), and so forth.

Mechanical properties of high-strength concrete incorporate copper slag as a fine aggregate and concluded that less than 40% copper slag as sand substitution can achieve high-strength concrete comparable to or better than the control mix, beyond which, however, its behaviors decreased significantly [1–3].

Glass fiber-reinforced concrete consists of high-strength, alkali-resistant glass fiber embedded in a concrete matrix. In this form, both fibers and matrix retain their physical and chemical identities, while offering a synergistic combination of properties that cannot be achieved with either of the components acting alone.

High-performance fiber-reinforced cementitious composites (HPFRCCs) [4, 5] are a group of fiber-reinforced cement-based composites which possess the unique ability to flex and self-strengthen before fracturing. Strain hardening, the most coveted capability of HPFRCCs, occurs when a material is loaded past its elastic limit and begins to deform plastically. This stretching or "straining" action

actually strengthens the material. The basis for the engineered design of different HPFRCCs varies considerably despite their similar compositions. For instance, the design of one type of HPFRCC called Engineered Cementitious Composite (ECC) stems from the principles of micromechanics. ECC, also called bendable concrete, is an easily molded mortar-based composite reinforced with specially selected short random fibers, usually polymer fibers [6, 7]. Unlike regular concrete, ECC has a strain capacity in the range of 3–7%, compared to 0.01% for ordinary Portland cement (OPC). ECC, therefore, acts more like a ductile metal than a brittle glass (as does OPC concrete), leading to a wide variety of applications [8, 9].

Ultrahigh-performance concrete (UHPC) is a new type of concrete that is being developed by agencies concerned with infrastructure protection [10–14]. UHPC is characterized by being a steel fiber-reinforced cement composite material with compressive strengths in excess of 150 MPa, up to and possibly exceeding 250 MPa. UHPC is also characterized by its constituent material make-up: typically fine-grained sand, silica fume, small steel fibers, and special blends of high-strength Portland cement. Note that there is no large aggregate. The current types in production differ from normal concrete in compression by their strain hardening, followed by sudden brittle failure. Ongoing research into UHPC failure via tensile and shear failure is being conducted by multiple government agencies and universities around the world.

The high-strength self-consolidating (self-compacting) concrete technology is made possible by the use of polycarboxylates plasticizer instead of older naphthalene-based polymers and viscosity modifiers to address aggregate segregation [15, 16].

Combination of microsilica and nanosilica (colloidal silica) is considered to design high-strength self-consolidating concrete [1, 20, 21]. The results also revealed that 7% substitution of microsilica showed the same effect as 2% nanosilica replacement [1, 22, 23].

The fiber-matrix interfacial transition zone (ITZ) at nanoscale plays an important role in determining the mechanical performance of hybrid steel-polypropylene fiber-reinforced concrete at upper scales. This topic [24] presents the elastic behavior of the ITZ between steel/polypropylene fiber and pure cement paste through nanoindentation for different water/cement ratios.

Thus, the fine-grained structure with high homogeneity is characterized by increase of the integrated strength between aggregate and cement stone and decrease of specific stress in the contact area. Adhesion of sand component increases significantly with increase of contact area; these conditions were realized when creating the fine-grained concrete based on composite binders by using crushed granite from Wrangel deposit (Russian Far East). The aim of the study was to develop the concrete matrix dense structure with high gas, water, and vapor impermeability. Composite binders, obtained by cogrinding of Portland cement, fly ash, crushed limestone, and superplasticizer, have been proposed to achieve this aim. One of the ways to improve the properties of concrete and to reduce permeability parameters is the use of highly active additives of various compositions and genesis at micro- and nanosized levels, which contribute to the optimization of structure formation processes by initiating the formation of hydrated compounds. The efficiency of use of the active mineral additives of nanostructured silica-modifier composition has been proven in topics [1, 20, 21, 23]. The possibility of the permeability reduction of the concrete by mechanically grinding the composite binders components was also studied previously [17]. However, the protective properties (impermeability parameters) and efficiency of high-density impermeable concrete (HDIC) produced on the basis of composite binder were not considered previously.

An assumption about the possibility of HDIC is obtained by varying the amount and type of additives, fineness of the composite binder components, and hardening conditions [18, 25]. The purpose of this work is to improve impermeability and strength characteristics of the fiber-reinforced concrete through use of composite binders obtained by cogrinding of Portland cement, superplasticizer, fly ash of a thermal power station, and crushing screenings limestone.

2. Materials and Methods

To achieve this goal, the following tasks were completed in this work:

(i) Study of mineral composition, particle size distribution, and physical and mechanical characteristics of the binders components and fillers for concrete

(ii) Research of the effect of mineral and organic additives on the properties of composite binders

(iii) Study of the properties of fiber-reinforced concrete, depending on the characteristics of the composite binder taking into account peculiarities of structure formation to improve the impermeability and strength characteristics, research on characteristics of water absorption and gas, water, and vapor permeability of developed concrete, and experimental industrial testing of the proposed compositions

The science work included grinding of composite binder components in a varioplanetary mill. Ordinary Portland cement (OPC), fly ash (FA), limestone crushing waste (LCW), and superplasticizer were used as ground components.

The chemical and mineralogical compositions of the raw materials obtained by means of X-ray florescence (on D8 ADVANCE powder diffractometer from Bruker AXS) are presented in Tables 1 and 2.

In the varioplanetary mill, the rotational speeds of the grinding jars and the support disc can be set completely independently. The movement and the trajectory of the grinding balls can be influenced by varying the gear ratio, so that the balls strike horizontally on the inner wall of the grinding jar (by high impact energy), approach tangentially (by high friction), or simply roll over the inner wall of the grinding jar (by centrifugal mills). All intermediate stages and combinations between pressure friction and impact can be freely set (Figure 1). Accordingly, grinding by the varioplanetary mills is more energy-efficient than that by the ball mills and the vibratory mills. In addition, due to the

Table 1: The chemical compositions of the fly ashes, Portland cement, and limestone crushing wastes.

The predominant type of coal	Fly ash				Portland cement	LCW
	Primorye TPP	Vladivostok TPP	Artem TPP	Partizansk TPP		
	Luchegorsk and Bikinsky	Primorsky brown (Pavlovsky section)	Coal	Neryungrinsky coal		
Content of elements in terms of oxides, %						
SiO_2	55.3	63	48.1	47.4	20.2–20.9	7.49
TiO_2	0.5	0.5	0	0.9		0.24
Al_2O_3	12.6	21.4	29.3	22.3	6.0–6.7	3.33
Fe_2O_3	10.7	7.5	6.5	19.6	3.5–4.0	0.24
CaO	12.5	3.4	9.7	4.8	66.2–67	44.21
MgO	3.5	2.1	1.8	2.8	1.4–2.0	2.57
K_2O	1	1.3	1.2	0.1		
Na_2O	0.4	0.3	0.2	0.4		
SO_3	3.4	0.6	2.3	1.62		
LOI	2.3	1.4	0.6	<5	0.18	38.71

Table 2: The mineral compositions of Spassky Portland cement.

Mineral composition	C_3S	C_2S	C_3A	C_4AF
Content [%]	58–67	8–15	10–12	10.5–12.5

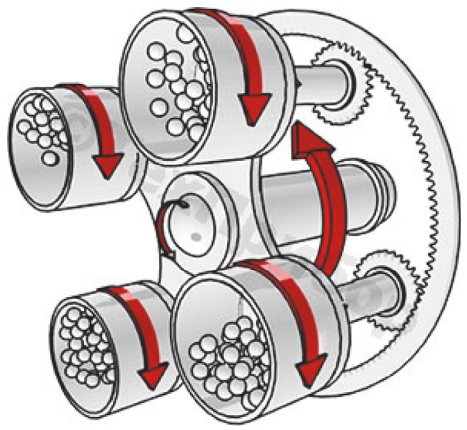

Figure 1: Operating principle of a varioplanetary mill.

joint action of shock, centrifugal shock, and abrasive forces, it becomes possible to achieve more highly disperse powders [26–29].

The reliability of results is provided by a systematic study with standard tools and methods for measuring, the mix of modern physical and chemical methods of analysis, X-ray diffraction and DTA, electron microscopy, and a sufficient amount of raw data and research results. The tasks of the scientific work were accomplished by implementing a systematic approach in the triad "composition (raw materials), structure, and properties" [30–32]. The studies were conducted with use of conventional physical-mechanical and physical-chemical methods of quality assessment of raw materials and synthesized materials as well as finished products.

The fly ashes of largest thermal power plants (TPPs) of Russia (Vladivostok TPP (Figure 2), Artem TPP, Primorye TPP, and Partizansk TPP) were used as components of composite binders. The important factor is the possibility of dry ash selection, which is currently realized for these TPPs.

Taking into consideration the fact that the focus of the paper is the development and use of environmentally friendly materials, the ashes' radioactivity has been evaluated (Table 3).

Thermal studies of the ash showed that, in the range of low temperatures, physically bound water is removed from it. Exothermic effect with the maximum at about 400°C indicates burnout of organic substances and endotherm effect at 712°C indicates dissociation of calcite to CaO and CO_2, which was confirmed by X-ray diffraction data (Figure 3).

Optimization of structure formation processes at hydration of the composite binder components creates the matrix dense structure which is necessary for creating increased impermeability composites. This can be realized by cogrinding of the Portland cement and the polyfunctional mineral admixtures and by reducing the concrete mix water-cement ratio through use of superplasticizers.

To reduce the water demand of concrete mix, the superplasticizers were used. They were selected of six most common construction material markets in the Far East. Cement paste shrinkage was measured by Hagerman cone. The Spassky cement CEM I 42.5N was used as grout. Water-cement ratio was 0.3. Plasticizer dosage was 0.3%. Time of measurement of shrinkage cone is recorded after the end of the cement paste mixing.

Achievement of high values of shrinkage cone is marked in the raw mix of binder and superplasticizer PANTARHIT PC160 Plv (Table 4).

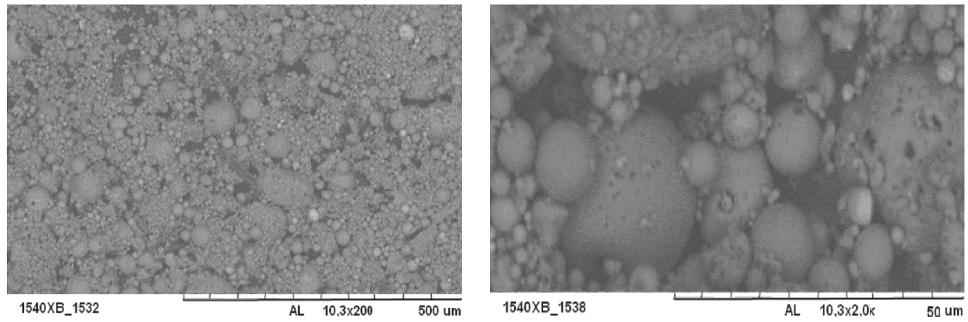

(a) (b)

Figure 2: The Vladivostok TPP's fly ash micrographs: (a) ×200; (b) ×2000.

Table 3: Specific effective activity of fly ash depending on the composition [19].

Name of indicator	The measurement result (A) [Bq/kg]			
	Primorye TPP	Vladivostok TPP	Artem TPP	Partizansk TPP
Activity ^{40}K	496.9 ± 101	362 ± 89	342 ± 68	516.9 ± 101
Activity ^{232}Th	153.6 ± 20.3	31.5 ± 19.7	29.5 ± 15.7	193.2 ± 22.3
Activity ^{226}Ra	163.1 ± 9.36	37.63 ± 6.32	27.23 ± 5.93	113.1 ± 6.37
$A_{\text{eff}} = A_{\text{Ra}} + 1.31A_{\text{Th}} + 0.085A_{\text{K}}$	>398	80 ± 30	93 ± 20	>410

Table 4: Shrinkage of the cement paste with different superplasticizers.

Time [min]	Melflux 1641 F	Melflux 5581 F	PANTARHIT PC160 Plv	FOX™-8H	PC-1030	JK-04 PPM
			Shrinkage [mm]			
0	290	350	370	250	240	130
5	380	390	400	260	280	120
30	390	350	390	240	190	98

Time: the time since beginning of measurement.

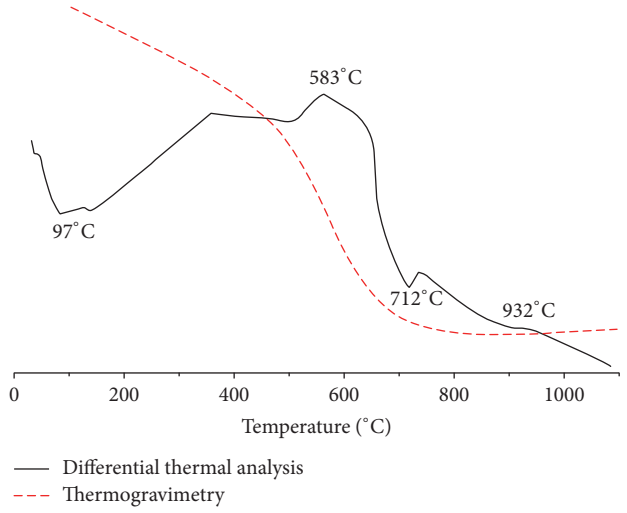

Figure 3: The DTA and TG results of the Vladivostok TPP fly ash [17–19].

The raw components were milled and mixed in various proportions (OPC 30–100%, FA 0–50%, LCW 0–20%, and superplasticizer 0.3%) in a varioplanetary mill for one hour. The materials mixing was carried out using cyclic and continuous flow dispensers with automatic control with a maximum weighing cycle duration of 45–90 s, with a weighing accuracy of 1–3%. All raw materials were dosed by mass, with the exception of water and liquid additives (if any) dosed by volume. In our research, there were no liquid additives. Water was added at the last stage, during the mortar preparation.

The control samples were made from a composite paste without addition of sand and fiber. Number of specimens was fabricated to determine the optimum composition of the binder.

The flowability of the concrete mix was evaluated using Hagerman cone molded from a concrete mix. Water-binder ratio was 0.3. The inverted cone was filled with a freshly prepared concrete mix without sealing. 90 seconds after filling, the cone rose upward. Immediately the stopwatch was turned on. As the mixture reached a diameter of 500 mm and also after the spreading process was completed, the time was fixed. After the flow was completed, the maximum diameter of the spread of the concrete mix was determined.

The compressive strength and the modulus of elasticity of the specimens were researched on 70 mm cubes at the 28th day; however, 100 × 100 × 500 mm prisms were prepared for four-point bending to obtain flexural strength of the

Figure 4: Bruker BioSpin NMR Spectroscopy.

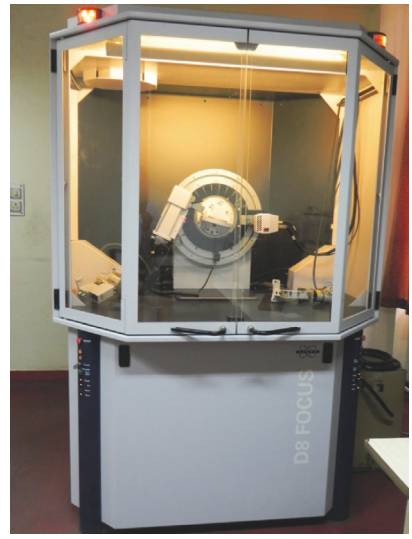

Figure 5: Bruker D8 ADVANCE powder X-ray diffractometer.

specimens with effective span of 400 mm. Mechanical tests were performed with Servo-hydraulic Fatigue and Endurance Tester Shimadzu Servopulser U-type with capacity of 200 kN and as per BS EN 12390-3:2002. The compressive strength was calculated as the arithmetic average of the six samples.

The porosity of the hardened specimens was determined on $1 \times 1 \times 3$ cm and $3 \times 3 \times 3$ cm specimens. The structure of the cement stone was investigated at the age of 28 days. The porosity was determined by a number of mutually complementary methods, namely,

(i) proton magnetic resonance with a pore measurement range of $1 \times 10^{-3} \cdots 1 \times 10^{-1}$ μm in diameter (using Bruker BioSpin NMR Spectroscopy (Figure 4));

(ii) small-angle X-ray diffraction with a measurement range of $2 \times 10^{-3} \cdots 3 \times 10^{-1}$ μm (on D8 ADVANCE powder diffractometer from Bruker AXS (Figure 5));

(iii) mercury porosimetry with a measurable range of $1 \times 10^{-1} \cdots 4 \times 10$ μm (using PoreMaster GT (Figure 6));

(iv) optical microscopy of thin sections with a measuring range of $4 \times 10 \cdots 1 \times 10^{3}$ μm.

X-ray phase analysis determined the degree of cement hydration and the content of low-base calcium hydrosilicates, CSH (I). The phases were identified by the international JCPDS table. The degree of hydration was determined from the intensity of the main C_3S reflex. The amount of CSH (I) was established by comparing the intensity of the main β-CS reflex obtained on samples of hardened cement sintered at 1000°C with a standard sample (quartz).

Figure 6: PoreMaster GT.

3. Experimental Part

Seven binder composites were developed for further research (Table 5). Superplasticizer PANTARHIT PC160 Plv at quantity 0.3% was added to each of them. The binder : sand ratio is 1 to 3. To determine the optimal dosage of components in the "cement-limestone-ash" system, it was necessary to grind them to specific surface of 600 m^2/kg at various ratios.

According to Table 5, positive dynamics of strength growth of the composite binder under the joint influence of the ash fine constituents, limestone crushing wastes, and superplasticizer with maximum increase in the activity of the binder at 62% were found.

This is due to the fact that active mineral components of the composite binder contribute to the binding of $Ca(OH)_2$ produced during cement hydration, which results in formation of additional amount of hydrosilicate neoplasms. At the same time, optimizing the process of structure formation is achieved by composite polydispersed components. Highly dispersed spherical ash particles act as crystallization centers

Table 5: Compositions and strength of composite binders.

Number	Cement content, by weight [%]	Fly ash content, by weight [%]		Limestone content, by weight [%]	Compressive strength [MPa]		
		Vladivostok TPP	Artem TPP		3 d.	7 d.	28 d.
1	100	—	—	—	17	32.5	47.5
2	30	—	50	20	30.2	40.1	50.4
3	35	45	—	20	34.2	43.1	53.2
4	40	—	45	15	36.6	48.2	56.6
5	45	45	—	10	39.2	50.1	59.2
6	50	—	40	10	45.1	54.9	65.8
7	55	40	—	5	47.2	54.1	70.2
8	100	—	—	—	60.3	81	103.2

Note. The prototype is number 1 (without final grinding); compositions numbers 2–8 are ground to S_{sp} = 600 m^2/kg.

Table 6: Bond between compressive strength [MPa] of the cement stone samples and the specific surface area of the composite binder [4].

Hardening time [d.]	Specific surface area of the composite binder [m^2/kg]					
	500	550	600	700	800	900
3	46.1	**47.4**	**47.2**	46.0	45.6	45.5
7	50.3	**54.2**	**54.1**	49.1	48.6	48.4
28	68.1	**77.3**	**70.2**	65.8	55.0	65.0

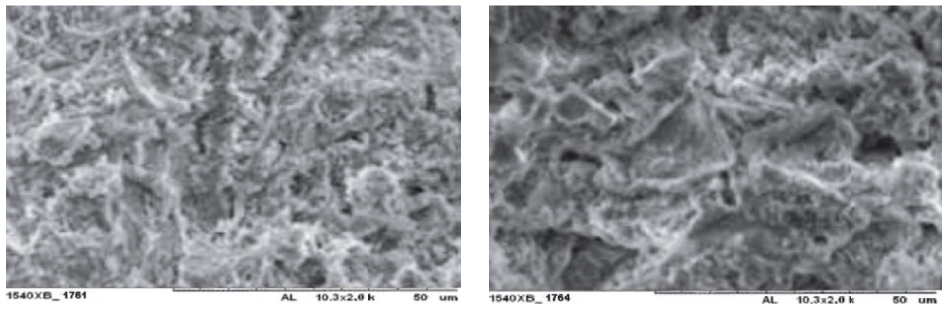

(a) (b)

Figure 7: The cement stone microstructure: (a) CEM I 42.5N based; (b) composite binder based (composition number 7 in Table 5).

and are used as filler at the nano- and microlevels. In conjunction with the larger particles of the mineral component, denser filling of intergranular spaces is noted in concrete cement stone structure with reduction in number of pores and microcracks.

This is confirmed by micrographs of composite cement paste derived by joint grinding of clinker and industrial wastes of the Russian Far Eastern region. Cement stone structure is very dense packing of small grains in the crystalline neoplasms total mass (Figure 7). The additional amount of hydrated crystalline phases contributes to filling of the voids at the microlevel in the crystalline matrix of calcium hydrosilicates at the boundary of the contact area, increasing adhesion degree of binder with filler.

In order to determine the optimum particle size, the Portland cement, the superplasticizer, the ashes, and the limestone were ground (dosage according to composite number 7 of Table 5) to different specific surface area (S_{sp}): 500, 550, 600, 700, 800, and 900 m^2/kg (Table 6).

According to Table 6, the 550–600 m^2/kg specific surface area (S_{sp}) of binder is optimal. Increasing S_{sp} above these values does not lead to further significant increase in strength. Reduction of start setting time of binder to 35–40 minutes by intensifying the hydration process under the influence of highly active components of the composite [17–19] should be noted.

Thus, the optimum parameters chosen for binder composition are specific surface area of 550 m^2/kg, the particle size of 0.15–500 microns, and average particle diameter of the grains of 0.65–11.2 mm [33, 34].

The most important task in creating HDIC is the rational formation and optimization of the pore space structure [35, 36]. In general, the overall reduction in porosity of compositions modified by the technogenic waste more than

Table 7: Influence of the composition of the composite binder to the cement stone porosity.

Composition according to Table 5	Porosity [%]			
	Technological (macroscopic level)	Capillary (microscopic level/submicroscopic level)	Gel (supramolecular level)	Total
1	1.2	4.6/2.3	8.2	16.3
2	2.6	1.7/4.5	1.6	10.4
3	1.3	1.1/5.0	3.5	10.8
4	1.4	1.9/2.3	4.4	9.6
5	3.6	1.7/2.5	1.6	9.4
6	3.2	1.1/1.0	3.5	8.8
7	1.0	0.9/1.8	4.4	8.1

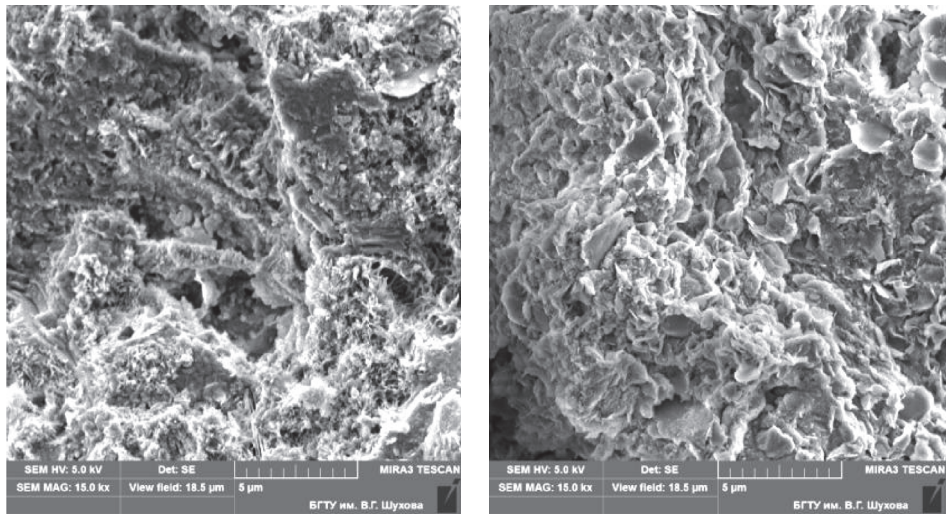

(a) (b)

Figure 8: The neoplasms micrographs: (a) cement stone without any additives; (b) cement stone based on composite binders.

2 times (from 16.3% to 8%) should be noted. Fluctuations of different diameter pores which depend on nature of their formation should also be noted (Table 7).

Existence of a large quantity of hydrosilicate connections is confirmed by decreasing of the gel pores in crystalline bunch in conjunction with modified composites on molecular level with porosity maximum reduction more than 5 times [37, 38]. Although the maximum strength is 77.3 MPa in the optimal composition of binder (by grinding to specific area of 550 m^2/kg), the gel porosity of the composite fell almost in 2 times. In this case, high strength is influenced by the complex actions: reduction of capillary porosity due to the intensification of the processes of growth of primary crystals of hydrosilicate phases [39, 40], due to possible formation of secondary recrystallization and crystals creation, due to filling the space at the micro- and submicrolevels of structural organization composite with them, and in conjunction with reduction technological porosity on 17% due to the formation of dense packing of the grain structure at the macrolevel, with the participation of spherical fine components of fly ash and limestone crushing wastes.

Denser structure of the binder composition with lower porosity is confirmed by microstructural studies. In phase of the modified binder formation, the amount of gel-like hydrate new formation increases on the surface of the filler particles (Figure 8(b)), there are no visible portlandite crystals, and it shows a decline of its share in the total mass of ligament hydrosilicate [41, 42].

By varying the percentage of added ash, it is possible to control number and size of ettringite crystals, which further define the properties of composite binder and concrete [43, 44]. The carbonates also have close contacts with cement stone, which is explained by the emergence of bonds between the cement hydration products and limestone [45, 46]. Growth of crystals of "needle-like" and "stem-like," low-basic hydrosilicates is observed [47, 48]; there are also plate-like calcium crystals, allegedly hydrocarboaluminates (Figure 8(b)), in the structure of the modified binder. Synthesis of these compounds is the result of interaction during hydration of clinker minerals $Ca(OH)_2$ with active mineral ingredients of ash and limestone [49, 50]. Growth of needle-shaped crystals contributes to reinforcement of the composite

structure on nano- and microlevels, reduction of porosity, and improvement of the composite complex strength [51, 52].

The greatest effect [53–55] is achieved through the synergistic impact of man-made pozzolanic additives (fly ash) and sedimentary-origin natural materials (limestone) at the content of OPC, 55 wt.%; LCW, 5 wt.%; and FA, 40 wt.%.

In this proportion, the composite material reaches the compressive strength of 77.3 MPa (by grinding to S_{sp} = 550 m^2/kg), at 45% replacement of cement with industrial waste. Thus, the effect of "cement, fly ash, and limestone" composite binder obtained by cogrinding with superplasticizer in the varioplanetary mill to structure formation process is determined. Ground active mineral supplements are the crystallization centers of neoplasms. Ash nanoparticles contribute to the binding of $Ca(OH)_2$, produced during the hydration of clinker minerals, intensifying binder hydration with forming needle-shaped crystals of low-basic hydrosilicate. Existence of the fine grains of limestone leads to forming hydrocarboaluminates. Implementation of the fiber-reinforced concrete potential is only possible by creating the material optimal structure, formation of which is determined by the following basic parameters: type and quality of raw materials, technology and preparation of concrete mixes, and quantitative relation between the components of fiber-reinforced concrete mixture.

4. Results and Discussions

Study of physical-mechanical properties of fine-grained concrete showed that use of the composite binder obtained by cogrinding of Portland cement, fly ash, limestone powder, and superplasticizer allowed increasing the compressive strength of fine concrete by 21%, while reducing almost in 2 times the proportion of cement. Prism strength and elastic modulus in the researched concrete types are significantly higher than in control samples (Table 8).

To optimize the fine-grained concrete structure forming on the macrolevel, steel fiber was used.

Taking into consideration previous studies [17–19], composition number 3 was adopted for the prototype (Table 8), to which fiber in an amount of 24 to 45 kg/m^3, that is, 2% of the total weight of the mixture in increments of 0.2%, was added. It was found that the structure optimization at the macrolevel improves the compressive strength by 24% (Table 9).

Addition of the domestically produced basalt fiber instead of the steel anchor fiber has not led to substantial improvement of physical and mechanical properties of concrete, so, for further investigations, fiber-reinforced concrete number 5 (1.6% reinforcement) is taken.

On basis of the research, it was revealed that the addition of the fly ash and the limestone waste to the composite binder promotes structural and phase changes in the formation of high-density composite impermeable structures.

The fine-grained fiber-reinforced types of concrete on the developed composite binder compositions number 2 and number 3 (Table 10), which achieve compressive strength of 100.2–100.9 MPa with the diffusion coefficient of $1.34 \cdot 10^{-4}$–$1.39 \cdot 10^{-4}$ cm^2/s, have the best physical and mechanical properties (Table 11).

It is revealed that, for fine-grained structure of concrete, in addition to high homogeneity, it is also characteristic to reduce specific stresses in the contact zone and increase the integral adhesion force between the cement stone and aggregate. The structure-forming role of the fine aggregate is most evident with an increase in the interaction surface; these conditions are realized in fine-grained types of concrete with the use of screening of granite crushed stone on the basis of composite astringents which, due to the highly developed surface, allow intensifying the processes of structure formation and accelerating the strength of concrete and also consolidating the structure.

As can be seen from the test results (Tables 10 and 11), composite binder of cement, fly ash from thermal power plants, and limestone at all dosages reduces the water permeability and air permeability of concrete. Thus, there is a clearly defined relationship between the properties of concrete and the features of the structure of cement stone: increasing the number of low-basic calcium hydrosilicates as well as increasing gel content and, correspondingly, reducing capillary porosity, especially at the submicroscopic level, predetermine the increase in strength and decrease in the permeability of concrete.

The maximum decrease in impermeability parameters was found in composition number 2 with the replacement of the proportion of cement in the binder mixture by 45% with the technogenic waste (FA and LCW). The air permeability of concrete decreased by 2 times (to 0.0253 cm^3/s), which according to GOST 12730.5 (Russian regulatory requirements) corresponds to mark W14 on permeability. The fiber-reinforced concrete's dense structure provides humidity resistance and reduces water absorption by volume in almost 2.5 times. These patterns are reflected in the water vapor permeability characteristics, which reaches the limit of 0.021 mg/(m·h·Pa) in the humid climate. The concrete's diffusion permeability was determined on the basis of data on the concrete neutralization rate (carbonation) by carbon dioxide in the absence of gradient of common air-gas pressure at the difference between the concentration of carbon dioxide in the concrete and that in environment at the time when the neutralization process is limited by the speed of carbon dioxide diffusion into the concrete porous structure. The experimental procedure is intended for use in the technology development and the designing of concrete compositions that provide long-term maintenance-free operation in the construction in nonaggressive and aggressive gas-air environment.

When evaluating the diffusive permeability, the average value of neutralized concrete layer thickness was found for all developed compounds. It was found that the developed concrete has an effective diffusion coefficient of $D' = 1.34 \cdot 10^{-4}$ cm^2/s.

Thus, the clear link between the concrete properties and characteristics of the cement stone structure (the increase in the number of hydrosilicate neoplasms) at the complex reducing of gel and capillary porosity is revealed, which

Table 8: Physical and mechanical properties of fine-grained concrete depending on the binder composition [25].

Composition numbers	Material consumption per 1 m^3								Compressive strength [MPa]	Prism strength [MPa]	Elastic modulus [MPa]
	Cementitious binder [kg]				Screenings of crushed granite [kg]	Sand [kg]	Water [l]	Slump [cm]			
	Cement	Fly ash	Limestone	Superplasticizer							
1*	550	—	—				220		107.5	86.3	61.2
2	288	235	27				240		83.7	59.5	43.8
3	275	246	29				241		84.2	60.3	44.5
4	257	257	36	1.2	1000	623	242	10–12	76.3	55.2	40.9
5	244	268	38				243		75.2	55.0	40.8
6	230	278	42				244		75.0	54.9	40.8
7**	550	—	—				215		63.1	42.3	36.2

*The binder of low water ratio with the specific surface of 550 m^2/kg. **The binder based on Portland cement CEM I 42.5N.

Table 9: Dependence of the strength of fiber-reinforced concrete on the percentage of reinforcement.

Composition numbers	Material consumption per 1 m^3				Reinforcement [%]	R_{compr}, [MPa]
	Binder [kg]	Water [l]	Aggregate [kg]	Fiber [kg]		
3-1*	550	240	1623	—	0	94.2
3-2	550	240	1623	23.97	1	96.1
3-3	550	240	1623	28.76	1.2	97.3
3-4	550	240	1623	33.56	1.4	99.8
3-5	550	240	1623	38.35	1.6	100.9
3-6	550	240	1623	43.15	1.8	99.5
3-7	550	240	1623	47.94	2	99.6

*Prototype composition corresponds to composition number 3 (according to Table 8).

Table 10: Compositions and strength characteristics of the fiber-reinforced concrete.

Number	Material consumption per 1 m^3						Slump [cm]	Prism strength [MPa]	Compressive strength [MPa]
	Cementitious binder [kg]				Aggregates [kg]	Water [l]			
	Cement	Fly ash	Limestone	Superplasticizer					
1	550	—	—	1.2	1623	220	10–12	66.3	115.5
2	288	235	27		1623	240		69.5	100.9
3	275	246	29		1623	241		70.3	100.2
4	257	257	36		1623	242		65.2	96.3
5	244	268	38		1623	243		65.0	95.2
6	230	278	42		1623	244		64.9	95.0

Table 11: The concrete performance characteristics depending on the binder composition.

Number (according to Table 10)	Air permeability of concrete a_c [cm^3/s]	Mark on water permeability, W	Effective diffusion coefficient [cm^2/s]	Water absorption by volume [%]	Vapor permeability [mg/(m·h·Pa)]	
					For dry climate	For wet climate
1	0.0565	W10	$1.56 \cdot 10^{-4}$	14.8	0.032	0.030
2	0.0253	W14	$1.34 \cdot 10^{-4}$	6.1	0.022	0.021
3	0.0289	W14	$1.39 \cdot 10^{-4}$	6.3	0.026	0.025
4	0.0402	W12	$1.64 \cdot 10^{-4}$	7.8	0.027	0.026
5	0.0465	W12	$1.79 \cdot 10^{-4}$	10.9	0.030	0.029
6	0.0423	W12	$1.82 \cdot 10^{-4}$	14.4	0.032	0.030

is especially observed at the molecular and submicroscopic levels determining the growth of strength and increase of concrete impermeability.

The approbation of theoretical and experimental studies is carried out on the example of monolithic fiber-reinforced concrete walls with permanent formwork developed by Fediuk et al. [18, 25, 56]. The thermal resistance of wall is R_o = 4,223 (m^2 ·°C)/W; the vapor permeability coefficient is μ = 0,021 mg/(m·h·Pa). The fiber-reinforced types of concrete developed on basis of the composite binder can be used in the construction of high-rise buildings [57].

The technological circuit production of the high-density fiber-reinforced concrete is developed. It comprises the following steps: cogrinding of Portland cement, fly ash, and limestone crushing waste; two-stage mixing with the filler and the fiber; filling of formwork; and mechanical compaction of the concrete mix. This production line can be implemented in cement plants in different regions.

Thus, the possibility of reducing permeability of fiber-reinforced concrete by varying the amount and type of additives and fineness and taking into account the conditions of curing is studied. It allows creating materials for multilayer load-bearing structures with a compressive strength of 100 MPa, with low permeability under actual operating conditions. Implementation of the research results will help to improve the environmental situation of regions, as fiber-reinforced concrete comprises 50–60% of industrial waste.

5. Conclusion

Positive dynamics of strength growth of the composite binder under the joint influence of the ash fine constituents, limestone crushing wastes, and superplasticizer with maximum increase in the activity of the binder at 62% were found. This is due to the fact that active mineral components of the composite binder contribute to the binding of $Ca(OH)_2$

produced during cement hydration, which results in formation of additional amount of hydrosilicate neoplasms. The overall reduction in porosity of compositions modified by the technogenic waste more than 2 times (from 16.3% to 8%) should be noted.

High strength is influenced by the complex actions:

(i) Reduction of capillary porosity due to the intensification of the processes of growth of primary crystals of hydrosilicate phases

(ii) Possible formation of secondary recrystallization and crystals creation

(iii) Filling the space at the micro- and submicrolevels of structural organization composite with them and in conjunction with reduction technological porosity on 17%

(iv) The formation of dense packing of the grain structure at the macrolevel, with the participation of spherical fine components of fly ash and limestone crushing wastes

The greatest effect is achieved through the synergistic impact of man-made pozzolanic additives (fly ash) and sedimentary-origin natural materials (limestone) at the content of OPC, 55 wt.%; LCW, 5 wt.%; and FA, 40 wt.%.

The fine-grained fiber-reinforced types of concrete on the developed composite binder, which achieve compressive strength of 100.2–100.9 MPa with the diffusion coefficient of $1.34 \cdot 10^{-4}$–$1.39 \cdot 10^{-4}$ cm^2/s, have the best physical and mechanical properties. As can be seen from the test results, composite binder of cement, fly ash from thermal power plants, and limestone at all dosages reduces the water permeability and air permeability of concrete.

Conflicts of Interest

The authors declare that they have no conflicts of interest.

References

[1] S. Chithra, S. R. R. Senthil Kumar, and K. Chinnaraju, "The effect of Colloidal Nano-silica on workability, mechanical and durability properties of High Performance Concrete with Copper slag as partial fine aggregate," *Construction and Building Materials*, vol. 113, pp. 794–804, 2016.

[2] K. S. Al-Jabri, M. Hisada, S. K. Al-Oraimi, and A. H. Al-Saidy, "Copper slag as sand replacement for high performance concrete," *Cement and Concrete Composites*, vol. 31, no. 7, pp. 483–488, 2009.

[3] W. Wu, W. Zhang, and G. Ma, "Optimum content of copper slag as a fine aggregate in high strength concrete," *Materials and Corrosion*, vol. 31, no. 6, pp. 2878–2883, 2010.

[4] H. Stang and C. Pedersen, "HPFRCC - extruded pipes," in *Proceedings of the 1996 4th Materials Engineering Conference. Part 1 (of 2)*, pp. 261–270, November 1996.

[5] P. Tjiptobroto and W. Hansen, "Tensile strain hardening and multiple cracking in high-performance cement-based composites containing discontinuous fibers," *ACI Materials Journal*, vol. 90, no. 1, pp. 16–25, 1993.

[6] V. C. Li, "From mechanics to structural engineering: the design of cementitious composites for civil engineering applications," *Structural Engineering/Earthquake Engineering*, vol. 10, pp. 37–48, 1993.

[7] M. Li and V. C. Li, "Rheology, fiber dispersion, and robust properties of engineered cementitious composites," *Materials and Structures/Materiaux et Constructions*, vol. 46, no. 3, pp. 405–420, 2013.

[8] J. Qiu and E.-H. Yang, "Micromechanics-based investigation of fatigue deterioration of engineered cementitious composite (ECC)," *Cement and Concrete Research*, vol. 95, pp. 65–74, 2017.

[9] H. Luo, Y. Wu, A. Zhao et al., "Hydrothermally synthesized porous materials from municipal solid waste incineration bottom ash and their interfacial interactions with chloroaromatic compounds," *Journal of Cleaner Production*, vol. 162, pp. 411–419, 2017.

[10] D.-Y. Yoo and N. Banthia, "Mechanical properties of ultra-high-performance fiber-reinforced concrete: A review," *Cement and Concrete Composites*, vol. 73, pp. 267–280, 2016.

[11] D.-Y. Yoo, N. Banthia, and Y.-S. Yoon, "Predicting service deflection of ultra-high-performance fiber-reinforced concrete beams reinforced with GFRP bars," *Composites Part B: Engineering*, vol. 99, pp. 381–397, 2016.

[12] J. Yang, H. Shin, and D. Yoo, "Benefits of using amorphous metallic fibers in concrete pavement for long-term performance," *Archives of Civil and Mechanical Engineering*, vol. 17, no. 4, pp. 750–760, 2017.

[13] D. Yoo, I. You, and S. Lee, "Electrical properties of cement-based composites with carbon nanotubes, graphene, and graphite nanofibers," *Sensors*, vol. 17, no. 5, p. 1064, 2017.

[14] M. Castellote, I. Llorente, C. Andrade, and C. Alonso, "Accelerated leaching of ultra high performance concretes by application of electrical fields to simulate their natural degradation," *Materiaux et Constructions*, vol. 36, no. 256, pp. 81–90, 2003.

[15] M. Tabatabaeian, A. Khaloo, A. Joshaghani, and E. Hajibandeh, "Experimental investigation on effects of hybrid fibers on rheological, mechanical, and durability properties of high-strength SCC," *Construction and Building Materials*, vol. 147, pp. 497–509, 2017.

[16] M. Sahmaran and I. O. Yaman, "Hybrid fiber reinforced self-compacting concrete with a high-volume coarse fly ash," *Construction and Building Materials*, vol. 21, no. 1, pp. 150–156, 2007.

[17] R. S. Fediuk, "Mechanical Activation of Construction Binder Materials by Various Mills," in *Proceedings of the All-Russia Scientific and Practical Conference on Materials Treatment: Current Problems and Solutions*, vol. 125, November 2015.

[18] R. Fediuk and A. Yushin, "Composite binders for concrete with reduced permeability," in *Proceedings of the International Conference on Advanced Materials and New Technologies in Modern Materials Science 2015, AMNT 2015*, November 2015.

[19] R. S. Fediuk and A. M. Yushin, "The use of fly ash the thermal power plants in the construction," in *Proceedings of the 21st International Conference for Students and Young Scientists: Modern Technique and Technologies, MTT 2015*, vol. 93, October 2015.

[20] M. Sánchez, M. C. Alonso, and R. González, "Preliminary attempt of hardened mortar sealing by colloidal nanosilica migration," *Construction and Building Materials*, vol. 66, pp. 306–312, 2014.

[21] M. H. Mobini, A. Khaloo, P. Hosseini, and A. Esrafili, "Mechanical properties of fiber-reinforced high-performance concrete

incorporating pyrogenic nanosilica with different surface areas," *Construction and Building Materials*, vol. 101, pp. 130–140, 2015.

[22] N. Ranjbar, A. Behnia, B. Alsubari, P. Moradi Birgani, and M. Z. Jumaat, "Durability and mechanical properties of self-compacting concrete incorporating palm oil fuel ash," *Journal of Cleaner Production*, vol. 112, pp. 723–730, 2016.

[23] A. Hendi, H. Rahmani, D. Mostofinejad, A. Tavakolinia, and M. Khosravi, "Simultaneous effects of microsilica and nanosilica on self-consolidating concrete in a sulfuric acid medium," *Construction and Building Materials*, vol. 152, pp. 192–205, 2017.

[24] L. Xu, F. Deng, and Y. Chi, "Nano-mechanical behavior of the interfacial transition zone between steel-polypropylene fiber and cement paste," *Construction and Building Materials*, vol. 145, pp. 619–638, 2017.

[25] R. Fediuk, "High-strength fibrous concrete of Russian Far East natural materials," in *Proceedings of the International Conference on Advanced Materials and New Technologies in Modern Materials Science 2015, AMNT 2015*, vol. 116, November 2015.

[26] R. Ibragimov, "The influence of binder modification by means of the superplasticizer and mechanical activation on the mechanical properties of the high-density concrete," *ZKG International*, vol. 69, no. 6, pp. 34–39, 2016.

[27] L. H. Zagorodnjuk, V. S. Lesovik, A. A. Volodchenko, and V. T. Yerofeyev, "Optimization of mixing process for heat-insulating mixtures in a spiral blade mixer," *International Journal of Pharmacy and Technology*, vol. 8, no. 3, pp. 15146–15155, 2016.

[28] R. A. Ibragimov and S. I. Pimenov, "Influence of mechanochemical activation on the cement hydration features," *Magazine of Civil Engineering*, vol. 62, no. 2, pp. 3–12, 2016.

[29] E. Glagolev, L. Suleimanova, and V. Lesovik, "High reaction activity of nano-size phase of silica composite binder," *Journal of Environmental and Science Education*, vol. 11, no. 18, pp. 12383–12389, 2016.

[30] S. L. Buyantuyev, L. A. Urkhanova, S. A. Lkhasaranov, Y. Y. Stebenkova, A. B. Khmelev, and A. S. Kondratenko, "The methods of receiving coal water suspension and its use as the modifying additive in concrete," in *Proceedings of the 12th International Conference Radiation-Thermal Effects and Processes in Inorganic Materials*, vol. 168, September 2016.

[31] S. L. Buyantuev, L. A. Urkhanova, A. S. Kondratenko, S. Y. Shishulkin, S. A. Lkhasaranov, and A. B. Khmelev, "Processing of ash and slag waste of heating plants by arc plasma to produce construction materials and nanomodifiers," in *Proceedings of the 12th International Conference Radiation-Thermal Effects and Processes in Inorganic Materials*, vol. 168, September 2016.

[32] A. P. Semenov, N. N. Smirnyagina, L. A. Urkhanova et al., "Reception carbon nanomodifiers in arc discharge plasma and their application for modifying of building materials," in *Proceedings of the 12th International Conference Radiation-Thermal Effects and Processes in Inorganic Materials*, vol. 168, September 2016.

[33] R. Chihaoui, H. Khelafi, Y. Senhadji, and M. Mouli, "Potential use of natural perlite powder as a pozzolanic mineral admixture in Portland cement," *Journal of Adhesion Science and Technology*, vol. 30, no. 17, pp. 1930–1944, 2016.

[34] M. Koniorczyk, D. Gawin, and B. . Schrefler, "Modeling evolution of frost damage in fully saturated porous materials exposed to variable hygro-thermal conditions," *Computer Methods Applied Mechanics and Engineering*, vol. 297, pp. 38–61, 2015.

[35] K. Marcin, "Coupled heat and water transport in deformable porous materials considering phase change kinetics," *International Journal of Heat and Mass Transfer*, vol. 81, pp. 260–271, 2015.

[36] A. Peschard, A. Govin, P. Grosseau, B. Guilhot, and R. Guyonnet, "Effect of polysaccharides on the hydration of cement paste at early ages," *Cement and Concrete Research*, vol. 34, no. 11, pp. 2153–2158, 2004.

[37] R. S. Fediuk and D. A. Khramov, "Research on porosity of the cement stone of composite binders," *Int. Res. J*, vol. 1, pp. 77–79, 2016.

[38] Z. Liu, Y. Zhang, and Q. Jiang, "Continuous tracking of the relationship between resistivity and pore structure of cement pastes," *Construction and Building Materials*, vol. 53, pp. 26–31, 2014.

[39] Z. Liu, Y. Zhang, G. Sun, Q. Jiang, and W. Zhang, "Resistivity method for monitoring the early age pore structure evolution of cement paste," *Journal of Civil, Architectural and Environmental Engineering*, vol. 34, no. 5, pp. 148–153, 2012.

[40] M. Schmidt, H. Pöllmann, A. Egersdörfer, J. Göske, and S. Winter, "Investigations on the puzzolanic reactivity of a special glass meal in a cementitious system," in *Proceedings of the 32nd International Conference on Cement Microscopy 2010*, pp. 86–118, 2010.

[41] M. Schmidt, H. Pöllmann, A. Egersdörfer, J. Göske, and S. Winter, "Investigations on the use of a foam glass containing metakaolin in a lime binder system," in *Proceedings of the 33rd International Conference on Cement Microscopy 2011*, pp. 319–354, 2011.

[42] A. Sachdeva, M. J. Mccarthy, L. J. Csetenyi, and M. R. Jones, "Mechanisms of sulfate heave prevention in lime stabilized clays through pozzolanic additions," in *Proceedings of the International Symposium on Ground Improvement Technologies and Case Histories, ISGI'09*, pp. 555–560, December 2009.

[43] A. J. Puppala, E. Wattanasanticharoen, V. S. Dronamraju, and L. R. Hoyos, *Ettringite induced heaving and shrinking in kaolinite clay*, vol. 162 of *Geotechnical Special Publication*, 2007.

[44] S. Liu and P. Yan, "Hydration properties of limestone powder in complex binding material," *Journal of the Chinese Ceramic Society*, vol. 36, no. 10, pp. 1401–1405, 2008.

[45] S. Liu and L. Zeng, "Influence of new admixtures on the properties of hydraulic concrete," *Journal of Hydroelectric Engineering*, vol. 30, no. 2, pp. 118–122, 2011.

[46] K. Pushkarova, K. Kaverin, and D. Kalantaevskiy, "Research of high-strength cement compositions modified by complex organic-silica additives," *EasternEuropean Journal of Enterprise Technologies*, vol. 5, no. 5, pp. 42–51, 2015.

[47] E. V. Fomina, V. V. Strokova, and N. I. Kozhukhova, "Application of natural aluminosilicates in autoclave cellular concrete," *World Applied Sciences Journal*, vol. 25, no. 1, pp. 48–54, 2013.

[48] K. Ma, J. Feng, G. Long, and Y. Xie, "Effects of mineral admixtures on shear thickening of cement paste," *Construction and Building Materials*, vol. 126, pp. 609–616, 2016.

[49] P. Shafigh, M. A. Nomeli, U. J. Alengaram, H. B. Mahmud, and M. Z. Jumaat, "Engineering properties of lightweight aggregate concrete containing limestone powder and high volume fly ash," *Journal of Cleaner Production*, vol. 135, pp. 148–157, 2016.

[50] A. Balza, O. Corona, A. Alarcón, J. Echevarrieta, M. Goite, and G. González, "Microstructural study of Portland cement additivated with Nanomaterials," *Acta Microscopica*, vol. 25, no. 1, pp. 39–47, 2016.

[51] F. Faleschini, M. A. Zanini, K. Brunelli, and C. Pellegrino, "Valorization of co-combustion fly ash in concrete production," *Materials and Corrosion*, vol. 85, pp. 687–694, 2015.

[52] B. Boulekbache, M. Hamrat, M. Chemrouk, and S. Amziane, "Flexural behaviour of steel fibre-reinforced concrete under cyclic loading," *Construction and Building Materials*, vol. 126, pp. 253–262, 2016.

[53] M. Rudzki, M. Bugdol, and T. Ponikiewski, "An image processing approach to determination of steel fibers orientation in reinforced concrete," *Lecture Notes in Computer Science*, vol. 7339, pp. 143–150, 2012.

[54] T. Ponikiewski, J. Gołaszewski, M. Rudzki, and M. Bugdol, "Determination of steel fibres distribution in self-compacting concrete beams using X-ray computed tomography," *Archives of Civil and Mechanical Engineering*, vol. 15, no. 2, pp. 558–568, 2015.

[55] R. S. Fediuk and D. A. Khramov, "Physical equipment spectroscopic study of coal ash," *Modern Construction and Architecture*, vol. 1, pp. 57–60, 2016.

[56] R. S. Fediuk, A. K. Smoliakov, R. A. Timokhin, N. Y. Stoyushko, and N. A. Gladkova, *Fibrous Concrete with Reduced Permeability to Protect the Home Against the Fumes of Expanded Polystyrene*, vol. 66 of *Materials Science and Engineering*, 2017.

[57] M. Quintard, "Transfers in porous media," *Special Topics and Reviews in Porous Media*, vol. 6, no. 2, pp. 91–108, 2015.